An Image Based Microtiter Plate Reader System for 96-well Format Fluorescence Assays

Durai Arun P [1], **Sankaran K** [2], **Muttan S** [1]

[1] Dept. Of Electronics and Communication Engineering, College of Engineering, Anna University, Chennai

[2] Centre for Biotechnology, Alagappa College of Technology, Anna University, Chennai

Abstract

Background: 96-well microtiter plate assay are becoming popular analytical procedures in laboratory and clinical practices generating a demand for microtiter plate readers. The present colorimetric and fluorimetric based microtiter plate reader are efficient in general applications such as measuring reflectance, absorbance, and optical density of reaction mixtures. However, a dedicated system incorporating automation and computational techniques in specific microtiter plate readers for Drug discovery and Microbial viability, provides portability and compatibility with high-throughput analysis at affordable cost.

Objective: To develop image-based reader system for semi-quantitative measurements of transport assay performed in microtiter plate. In this work, we focus on deduction of illumination source and classification of fluorescence emitted by transport assay using this microtiter plate reader.

Method: We have taken the images of 96-well fluorescence efflux assay and developed an appropriate image analysis system to read the individual well images and categorize the results as fast efflux and slow efflux by the classifier. The images exhibited non-uniform illumination due to UV transilluminator, which then replaced by the circuit of blue LED after performing a study on its classification performance. Statistical descriptive features extracted from the image are classified using k-means clustering technique. The proposed system can be adapted to read any kind of microtiter plate assay.

Results: For uniform illumination of the source, of both UV transilluminator and blue LED, the color profile varied in accord to reaction mixture concentration. For classification performance of the source, out of four different images at various intensities of illumination from blue LED circuit controlled by potentiometer, the classification of efflux assay for image with maximum intensity gave high accuracy than the rest. For classification performance of the classifier, out of 1920-sub-images, the classifier misclassifies none.

Conclusion: For the microtiter plate reader, which classifies the liquid transport assay as fast efflux or slow efflux, the usage of UV transilluminator as illumination source is limited due to its non-uniform illumination and blue LED is apt for this application due its uniformity. The k-means clustering technique had been effective for this application when fed with statistical features describing the clusters.

Keywords

Microtiter plate reader, microtiter plate, fluorescence assay

Correspondence to:

S. Muttan
Department of Electronics and Communication Engineering
Address: College of Engineering, Guindy, Chennai – 600 025
E–mail: muthan_s@annauniv.edu

EJBI 2013; 9(2):58–68
received: January 31, 2013
accepted: April 17, 2013
published: August 30, 2013

1 Introduction

Fluorescence is becoming a popular optical method of chemical and biochemical analyses. Research laboratory and Clinical laboratory procedures increasingly make use of such methods. In this scenario, 96-well and 384-well based high-throughput assays are useful in drug discovery, microbial viability etc. The commercially popular readers that depends on the individual well reading during X-Y scanning is expensive and seriously limits the use of this method for peripheral clinical facilities. Hence, there is a need to develop instrumentation for microtiter plate reader.

In a typical microtiter plate based fluorescence assays in use, the reaction mixture is excited with a wavelength which is in the far UV or Visible region and the emission is measured in the visible range. In recent times, both excitation and emission are preferred in the visible range to reduce cost drastically, as LED sources have become very cheap. Scanning mode in commercial machines is the

one where the machines performs X-Y scan on each well of the microtiter plate and profile the fluorescence, absorbance, optical density, and other methods of the assay either by the pre-defined protocols or user-defined protocols. Hence, imaging mode would provide further advantage of cost and high throughput, than scanning mode of reading. There are several image analysis techniques used as in microscopy and gel documentation, but using that along with specific image acquisition for fluorescence or colorimetric assays in 96-well microtiter plate is the new venture. The available image acquisition system can be readily adapted for the microtiter plate imaging, but one has to develop appropriate statistical and computational methodologies for analyzing the data and convert the signal into useful outcome like concentration of an analyte or rate of reactions or positive or negative. The requirements for image acquisition hardware and image analysis systems could differ according to the need of application [1].

The goal of the proposed reader system is to group the samples in the image of 96-well microtiter plate assay in any one of the two categories, based on the assay performed. Gonzalez [2] and Shalkoff [3] have described in detail identifying a pattern recognition problem and providing the solution to it, which in this case, is a two-class pattern recognition problem. Statistical classification [4] can classify a two-class pattern recognition problem efficiently when apt features form the feature space. The challenge lies in finding the features, which shows the discrimination of classes. The computational technique [5] of extracting the useful features of the image helps in the process of feature selection.

The proposed system has a wide area of application for the assays performed in the 96-well microtiter plate when the developed algorithm is adapted for requirements of various assays. This enables the feasibility of a reader system being fast, accurate, and adaptive to various environments.

2 System Architecture

The Image analysis system developed to read the 96-well microtiter plate has sub-systems as any computer vision system [6] such as image acquisition, image preprocessing, image segmentation, feature extraction, and classifier. Here, the assay will provide the fluorescence difference when illuminated by UV-light or by any blue source in accord to the transport efflux. Wells' fluorescence is classified either fast or slow efflux individually by the classifier. As in [7], the architecture of the proposed reader has image acquisition hardware and image analysis software. The system architecture had underwent changes with respective to the changes evolved in the requirements of both in hardware and software. The system as in [7] had the hardware wherein there was no optic system for the magnification whereas an optic system is included for this proposed imaging hardware. Moreover, usage of UV transilluminator contributed non-uniform illumination over a single microtiter plate, which led to the idea of altering the source. In addition, we changed the number of classes from four to two for the classification, due to the incorporated changes in assay. The assay now focuses only to find, whether the sample shows a fast or slow efflux. The image acquisition hardware [8] consists of the source and the lens system to bring actual size of plate to the corresponding image size in the acquired image. The image of the microtiter plate acquired by the digital camera, led to limited usage of the image pre-processing, for now. The image segmentation sub-system's goal is to segment the single microtiter plate image into 96 sub-images. The feature extraction sub-system extracts the radiometric and densitometric features [9] of the fluorescence sub-images. The classification and the decision-making subsystem used is k-means clustering technique.

3 Methodology

3.1 Image Acquisition and Segmentation

The image acquisition hardware used here is to acquire the image of 96-well microtiter plate consists of a source and three-lens system [8]. The source excites the samples in the well when incident from below. The excitation wavelength to read the fluorescence of the samples in assay used by fluorometer is 485 nm. The source wavelength needed to excite the fluorescence assay lies in the blue region of visible spectrum. Hence, the image acquisition hardware of this system needs a UV transilluminator or Dark reader transilluminator or blue light emitting diode (LED) [10] as a source. The three-lens system used here is to bring the actual size of the object, here the microtiter plate, to the image size of the object in the image. The three-lens arrangement is plano-convex lens, plano-convex lens, and plano-concave lens. From the plano-concave lens, a digital camera acquires the input image. An offline transfer of image was done from camera to computer for further processing.

The image segmentation in this application needs to be highly accurate since the region of interest is all over the spatial area of the image. For feature extraction and classification, the system has to segment 96 individual wells from the single microtiter plate image. The image of 96 well plate assay acquired by any source shows the order of arrangement of wells having 8 rows and each row having 12 wells in it. The wells are cropped by finding the center pixel of the respective wells and index of each wells are assigned to the subscripts of 8 rows - 12 columns matrix dimension. Figure 1 shows the UV excited plate and blue light emitting diode excited plate along with its segmented images respectively.

The UV transilluminator provides UV light as excitation source and for blue light, a circuit was built with commercially available blue light emitting diode (LED) such as SMD 3528, which emits a narrow band of blue light

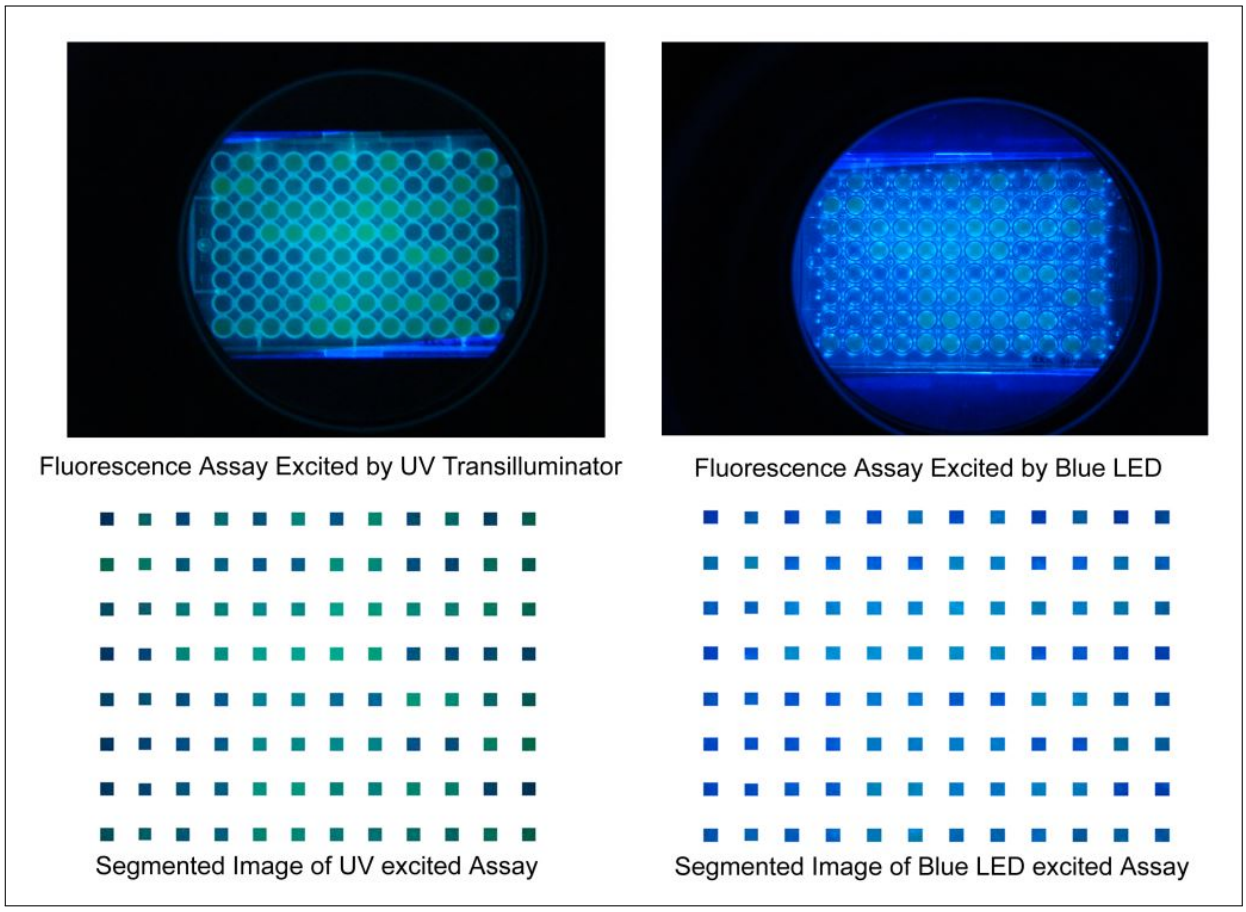

Figure 1: Original and Segmented Images of Fluorescence Assay excited by UV Transilluminator and Blue LED.

from 445 nm to 495 nm with center wavelength 470 nm. With the viewing angle of 120 degrees, the maximum luminous intensity range of 3528 blue LED is 600mcd and the maximum forward voltage range is 3.6V. The designed circuit delivers the maximum luminosity emitted per LED. Six LEDs per length and three LEDs per breadth are connected, making the arrangement that two lengthier sides have six LEDs each and two shorter sides have three LEDs each. Hence, the total luminance provided by this source is 100cd/m^2. Figure 2 shows the 3528 SMD blue light emitting diode source circuit designed for the 96-well microtiter plate to read the fluorescence assay.

Analysis of the illumination uniformity provided by the source over all wells of a plate shows its suitability for this application. An assay of fluorescein samples of concentration ranging from 100 nM to 5000 nM is prepared. The variation in the concentration of the fluorescein dye simulates the fluorescence emitted by the living microorganism samples. The lower the concentration the more blue the image will be and the higher the concentration the more green the image will be. The fluorescence assay is prepared in an arrangement such that every row and column has samples of different fluorescein concentration. This arrangement paved the way for the analysis of color definition of different concentration to different position of wells. Figure 3 shows the green component profile of plate bearing different concentration irrespective of the position of wells excited by UV and blue LED.

The characterization of the fluorescein sample is to show higher green component for higher concentration and should decrease as the fluorescein concentration lowers. On comparing the profiles of UV excitation and blue LED excitation as shown in Figure 3, only the blue LED excitation depicts the needed characterization. The variation in the green component profile of UV excited plate is due to the arrangement of the quartz tubes present in the UV transilluminator [11]. The blue LED source unlike the transilluminator provided a uniform illumination across the area beneath the plate and excites all wells with it; hence, the color definition did vary in accord to the fluorescein concentration of the samples, irrespective to the position of the wells. Therefore, the 3528 blue LED is the suitable source than UV transilluminator for this fluorescence reading application.

3.2 Feature Extraction

Feature extraction is the process of extracting the information, which forms the input vector for the classification engine. Nevertheless, this process is pre-ponded by Feature selection, an analytic process that provides the suitability of a data as an element of the input vector.

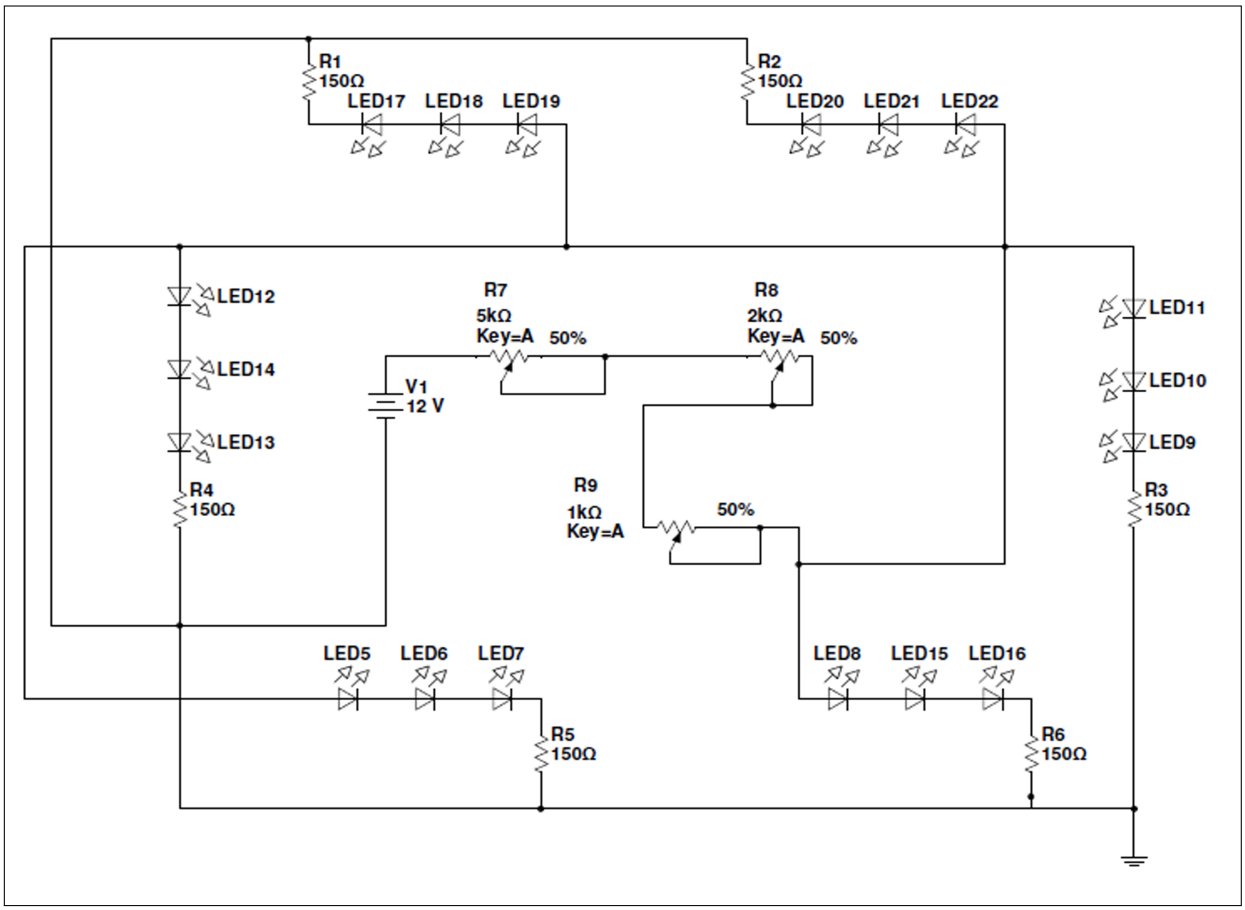

Figure 2: Schematic of Circuit designed with SMD3528 LED as Source for the Reader System.

Metin et al [9] have discussed the possible features which could be extracted from a fluorescence emitting images. The Chromatin specific features are the area of objects, integrated optical density, mean optical density, number of regions, compactness, distance, and center of mass. The radiometric and densitometric features are image bands, intensity, optical density, and mean optical hue. Statistical descriptive features, such as mean, median, mode, maximum, and minimum from the optical intensity of the pixels within the boundary pixels of the sub-images representing wells are extracted. Before performing the feature extraction and classification, in accord to the assay, segmented sub-images are re-assigned. The assay performed in the 96-well plate, from Test 1 to Test 6 forms six groups of samples, grouped as six different datasets for classification. The numbering inside the fields is the indexing of the wells of a 96-well plate in accord to the test performed. Table 1 shows the indices of segmented sub-images reassigned as in the assay template for feature extraction and classification. After finding the suitable features for this application, the classifier classifies the generated feature vector.

The color variation is the most important event in this application and any variability in intensity will affect the system's performance. The acquired image and segmented sub-images are RGB color space based image. The RGB color space is a three dimensional space, which has highly correlated Red (R), Green (G) and Blue (B) color vectors. The high correlation here means that if the intensity changes, all three-color vector components will change accordingly, known as 'Brightness Effect' [12]. For feature vectors, the red, green, blue components are less suitable, since visual enhancement is the focus of RGB color space than image analysis. The measurement of a color in RGB space does not represent color differences in a uniform scale, which reduces the possibility of evaluating the similarity of two colors from their distance in RGB space. The transformation of sub-images from RGB color space to HSV color space [12], converts the high correlative data to less correlative data. The HSV color space is also a variant of HSI (Hue-Saturation-Intensity) color space system.

The HSV color space system separates the color information and the intensity information from the image where, Hue and Saturation describes the Color Information and Value describes the Brightness Information. Hue represents the basic colors and Saturation is the measure of purity of color, which signifies the amount of white light mixed with the Hue. The Hue in HSV modeled from the Hue Color Wheel, defines any color in accord to its angle in the wheel. The angle range for Green and Blue in the Hue Color Wheel is 70 to 160 degrees and 165 to 240 de-

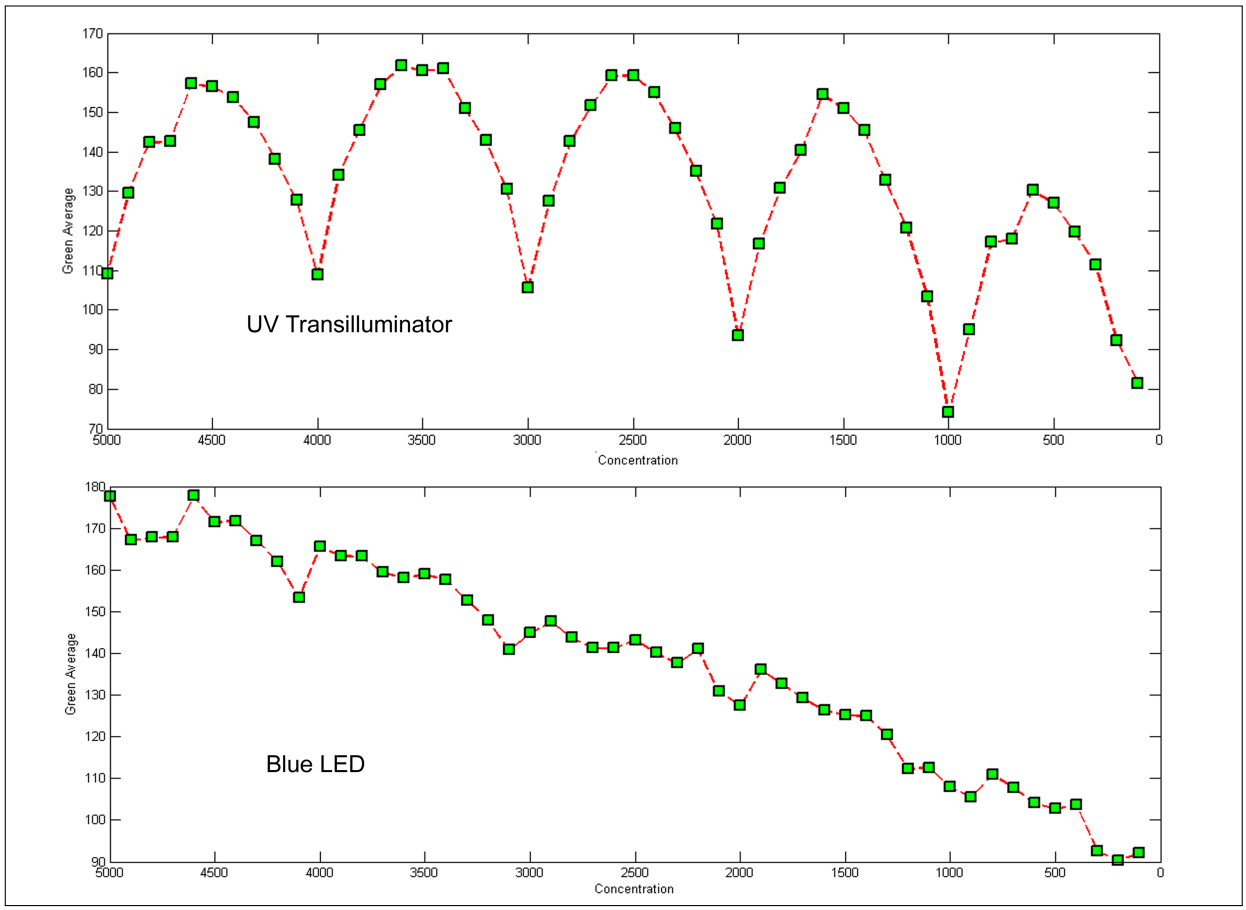

Figure 3: Green Component Profile for different concentration and positions excited by UV Transilluminator and Blue LED.

grees respectively. In HSV color space, the Hue range of Green and Blue is 0.2 to 0.4 and 0.45 to 0.7 respectively.

A fluorescein dye concentration simulates the color variation depicted by the fluorescent transport liquid assay. Assays of fluorescein concentrations 100 nM, 500 nM, 1000 nM, 2500 nM, and 5000 nM are prepared in five different plates, filled in all wells, and excited by blue LED. The color definition depicted due to fluorescence emitted by 1000 nM fluorescein concentration is the minimum for a fast transport efflux and fluorescence emitted by other lower concentration than 1000 nM depicts the color definition of slow transport efflux. Figure 4 shows the Hue average profile for different concentration, describing the curves descending from blue region to green region of the Hue in HSV in accord to its corresponding concentration. The Hue profile shows the variation corresponding to the concentration leading to its suitability as feature.

The developed system extracts color intensities from the Hue component of segmented sub-images as features. The features extracted are mean, median, mode, maxi-

Table 1: Template for Fluorescence Transport Liquid Assay in 96-well format.

Assay	Test 1		Test 2		Test 3		Test 4		Test 5		Test 6	
Plate Columns Plate Rows	1	2	3	4	5	6	7	8	9	10	11	12
A	1 (B)*	2 (C)♯	1 (B)*	2 (C)	1 (B)*	2 (C)♯	1 (B)*	2 (C)♯	1 (B)*	2 (C)♯	1 (B)*	2 (C)♯
B	3	4	3	4	3	4	3	4	3	4	3	4
C	5	6	5	6	5	6	5	6	5	6	5	6
D	7	8	7	8	7	8	7	8	7	8	7	8
E	9	10	9	10	9	10	9	10	9	10	9	10
F	11	12	11	12	11	12	11	12	11	12	11	12
G	13	14	13	14	13	14	13	14	13	14	13	14
H	15	16	15	16	15	16	15	16	15	16	15	16

*B – Blank ♯C – Control

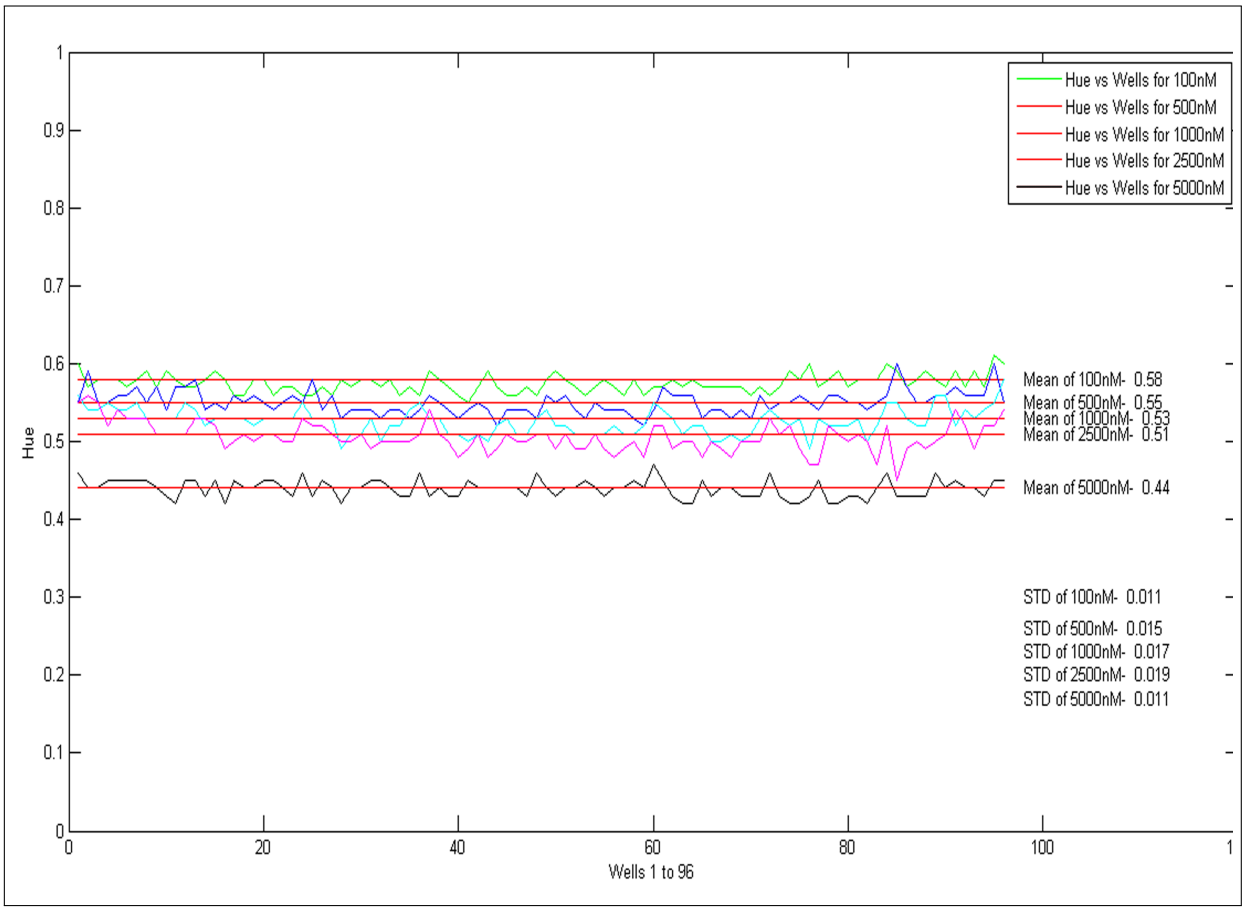

Figure 4: Hue Profile for Different Fluorescein Concentration in nanomolar excited by BLue LED.

mum, and minimum are represented as f_{me}, f_{md}, f_{mo}, f_{ma} and f_{mi} respectively. With image I of size $m * n * p$ and segmented into sub-images of $H\{s\}$, where H represents the cell array, m represents rows, n represents columns, p represents pages which corresponds to their components and s represents the index of the sub-images, the reader calculates the features. T_1, T_2, T_3, T_4, T_5, and T_6 represents the test groups re-assigned from the single cell array of $H\{s\}$ having a dataset of 16 sub-images in each groups. The index of the test groups is represented by t, which varies from 1 to 16 and not exceeding that. In the 3-page matrix of the HSV sub-images, converted from the 3-page RGB sub-images, the first page of HSV sub-image where $p = 1$ in the matrix $m * n * p$, is the Hue component represented as $T\{t\}(x, y, 1)$ where T is any test group. The x and y represents rows and columns of the segmented sub-images. The formula to calculate mean is given in equation (1).

$$f_{me} = \frac{1}{t}\sum_{t=1}^{16}\left[T\{t\}(x, y, 1)\right]. \tag{1}$$

For median (f_{md}), the data are sorted in ascending or descending order, and is calculated using equation (2).

$$f_{md} = \sum_{t=1}^{16}\frac{1}{2}\left[T\left\{\frac{t}{2}\right\}(x, y, 1) + T\left\{\frac{t}{2}+1\right\}(x, y, 1)\right]. \tag{2}$$

Mode (f_{mo}) as feature extracted from sub-images by formula as in equation (3) where, l is the lower limit of modal class, F_m is the frequency of modal class, F_{pm} is the frequency of class preceding the modal class, F_{cm} is the frequency of class succeeding the modal class, h is the size of class interval. The above mentioned parameters are derived from $T\{t\}$.

$$f_{mo}(t) = l + \left(\frac{F_m - F_{pm}}{2F_m - F_{pm} - F_{cm}}\right) * h. \tag{3}$$

The features maximum (f_{ma}) and minimum (f_{mi}) are obtained from the equations (4) and (5) respectively.

$$f_{ma}(t) = \max_{t=1\text{ to }16}\left(T\{t\}\right). \tag{4}$$

$$f_{mi}(t) = \min_{t=1\text{ to }16}\left(T\{t\}\right). \tag{5}$$

The feature space is the vital factor, which determines the efficiency of the classifying system. Hence, analyzing the extracted statistical descriptive features of Hue by using different combination of the features and viewing it

in its feature space gives the suitability of the features as input feature vector in this classification. Figure 5 shows sample of different feature spaces of a test group in single image of microtiter plate generated. The implementation of k-means clustering for features in different feature spaces in an image comprising of six test groups, tested the stability of the cluster formation leading to the deduction of feature space for classification. The measure used in this deduction was, inter and intra cluster distance obtained from the clustering and comparing the labels of sub-images with assay template. From all other feature spaces, we found that the maximum-minimum feature space with maximum of Hue of a sub-image as feature vector 1 and minimum of Hue of a sub-image as feature vector 2 gives the feature space suitable for an efficient classification by giving us distant clusters with limited over-fitting when analyzed with other images.

3.3 Classification

A classification technique depends on the requirements of the pattern recognition problem. In this application, the problem definition of pattern recognition is, it has two-class classification with only optical intensity of sub-images as data to extract the feature. The optical intensity tends to vary at all times since living microorganism is used in the fluorescence transport liquid assay which reduces the probability of estimating the variation contributed by it. Due to this problem, a fixed threshold or adaptive threshold based classification for this two-class classification is not possible when live samples contribute to the unpredictable variation in data. Since this is a two-class classification, a minimum distance classifier [13] when fed with effective features that depicts distinct clusters is enough. However, high throughput analyses are in need in selecting such features which does not deviate even when there is variability introduced by the living microorganism. The classification technique here used is the k-means clustering technique [14].

The k-means clustering algorithm aims to minimize the objective function as in (6) defined by the distance metric of a data point and its corresponding cluster center. The distance measure used in this application is Squared Euclidean Distance.

$$J = \sum_{j=1}^{k} \sum_{i=1}^{n} \|x_i^{(j)} - c_j\|^2 \qquad (6)$$

The $\|x_i^{(j)} - c_j\|^2$ is the chosen distance measure between a data point $x_i^{(j)}$ and the corresponding cluster center c_j. The k-means algorithm is composed of the following steps:

1. Initialize k center locations (i.e., $c_1, \ldots, c_k$);
2. Assign each $x_i^{(j)}$ to its nearest cluster center c_j.
3. Update each cluster center c_j as the mean of all $x_i^{(j)}$ that have been assigned closest to it.
4. Recalculate the positions of the k centers.
5. Repeat steps 2, 3, and 4 until the centers no longer move. This produces a separation of the objects into groups from which the metric to be minimized can be calculated.

K-means clustering are widely used for image segmentation and when incorporated with feature sets it can classify [15, 16, 17]. The classification process for this application starts from the acquisition of assay in microtiter plate as an image I of size $m*n*p$. Then, the application segments single image into 96 sub-images and place it in the cell array $H\{s\}$. The $H\{s\}$ is re-assigned in accord to the assay template into six groups $T1\{t\}$, $T2\{t\}$, $T3\{t\}$, $T4\{t\}$, $T5\{t\}$, and $T6\{t\}$, with t being index of sub-images in test groups.

The application transforms these test groups from RGB color space to HSV color space and represented as $TH1\{t\}$, $TH2\{t\}$, $TH3\{t\}$, $TH4\{t\}$, $TH5\{t\}$, and $TH6\{t\}$. As discussed in Section 3.2, hue component from the HSV sub-images, represented as $TH1\{t\}(x, y, 1)$, $TH2\{t\}(x, y, 1)$, $TH3\{t\}(x, y, 1)$, $TH4\{t\}(x, y, 1)$, $TH5\{t\}(x, y, 1)$, and $TH6\{t\}(x, y, 1)$ for all the test groups.

Maximum-minimum features forms the feature space extracted by the formulae as in (4) and (5) for the classification. $f_{ma}^{TH1}\{t\}$, $f_{ma}^{TH2}\{t\}$, $f_{ma}^{TH3}\{t\}$, $f_{ma}^{TH4}\{t\}$, $f_{ma}^{TH5}\{t\}$, and $f_{ma}^{TH6}\{t\}$ represents the maximum of Hue for test groups $TH1\{t\}$, $TH2\{t\}$, $TH3\{t\}$, $TH4\{t\}$, $TH5\{t\}$, and $TH6\{t\}$ respectively, whereas, $f_{mi}^{TH1}\{t\}$, $f_{mi}^{TH2}\{t\}$, $f_{mi}^{TH3}\{t\}$, $f_{mi}^{TH4}\{t\}$, $f_{mi}^{TH5}\{t\}$, and $f_{mi}^{TH6}\{t\}$, represents the minimum of Hue for the same. $F1\{t\}$, $F2\{t\}$, $F3\{t\}$, $F4\{t\}$, $F5\{t\}$, and $F6\{t\}$ represents the feature space of $TH1\{t\}$, $TH2\{t\}$, $TH3\{t\}$, $TH4\{t\}$, $TH5\{t\}$, and $TH6\{t\}$ respectively, generated as per general expression $F \rightarrow f(v, w)$ where F is the feature space, $f(.,.)$ is the function for feature elements v and w.

The function used in this application is to assign the f_{ma} features as x-axis elements and f_{mi} as y-axis elements in the feature space of F. Hence, $F1(t) \rightarrow f(f_{ma}^{TH1}\{t\}, f_{mi}^{TH1}\{t\})$, $F2(t) \rightarrow f(f_{ma}^{TH2}\{t\}, f_{mi}^{TH2}\{t\})$, $F3(t) \rightarrow f(f_{ma}^{TH3}\{t\}, f_{mi}^{TH3}\{t\})$, $F4(t) \rightarrow f(f_{ma}^{TH4}\{t\}, f_{mi}^{TH4}\{t\})$, $F5(t) \rightarrow f(f_{ma}^{TH5}\{t\}, f_{mi}^{TH5}\{t\})$, and $F6(t) \rightarrow f(f_{ma}^{TH6}\{t\}, f_{mi}^{TH6}\{t\})$.

These form as input to the k-means clustering with the two as number of clusters for each test group classification, represented by R for fast efflux and S for slow efflux for this application. $OH1\{t\}, OH2\{t\}, OH3\{t\}, OH4\{t\}$, $OH5\{t\}$, and $OH6\{t\}$, represents six different test output variables for the test groups $TH1\{t\}$, $TH2\{t\}$, $TH3\{t\}$, $TH4\{t\}$, $TH5\{t\}$, and $TH6\{t\}$, respectively. Let us represent k-means clustering based classification algorithm as a function whose notation is as in (7).

$$Label = Kmeans(F, n) \qquad (7)$$

where, $Label$ is the cluster label index assigned to data index, by the clustering technique, $Kmeans$ represents the

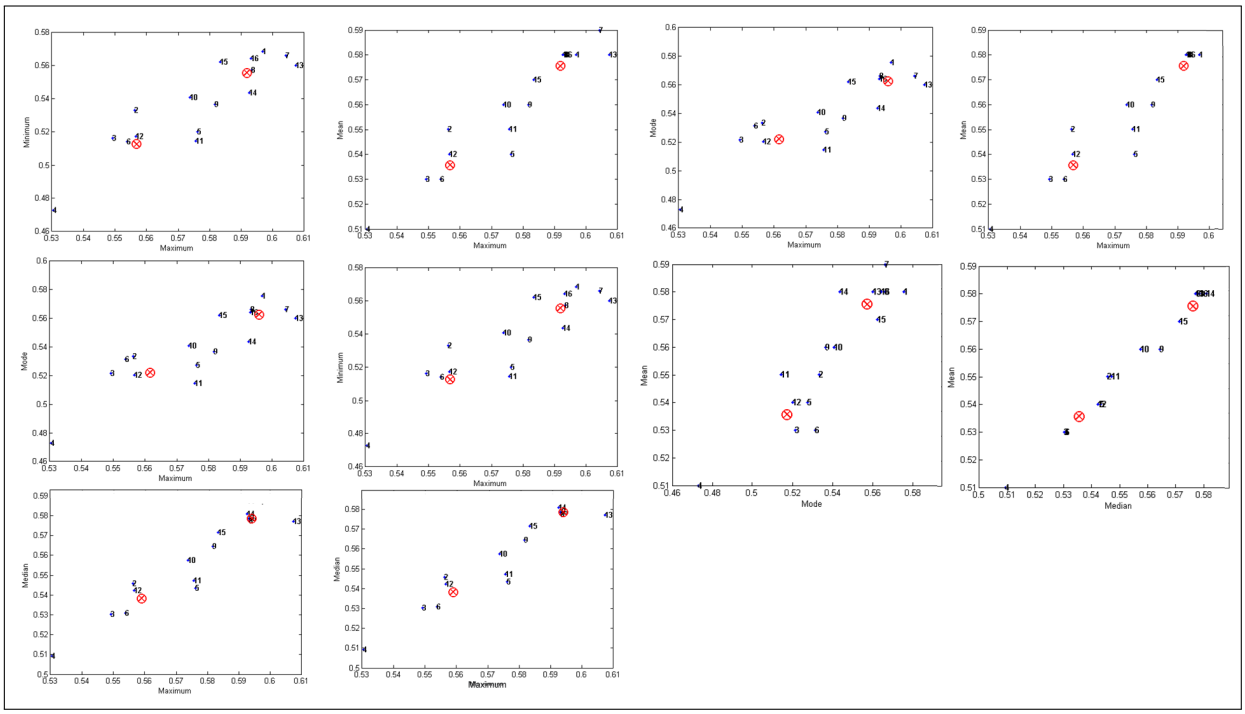

Figure 5: Different Feature Spaces Generated for Feature Selection.

function, F, the feature vector and n is the number of clusters. The application uses the above function for all test groups and obtains the cluster index.

$$OH1\{t\} = Kmeans(F1(t), 2) \quad (8)$$
$$OH2\{t\} = Kmeans(F2(t), 2) \quad (9)$$
$$OH3\{t\} = Kmeans(F3(t), 2) \quad (10)$$
$$OH4\{t\} = Kmeans(F4(t), 2) \quad (11)$$
$$OH5\{t\} = Kmeans(F5(t), 2) \quad (12)$$
$$OH6\{t\} = Kmeans(F6(t), 2) \quad (13)$$

The characters 'R' or 'S' representing fast and slow efflux respectively, replaces the index of the output variable of a single test assigned by k-means clustering. For each test, the classification gives output variables, which then re-assigned with indices along with content to a single cell array. $OH1\{t\}$, $OH2\{t\}$, $OH3\{t\}$, $OH4\{t\}$, $OH5\{t\}$, and $OH6\{t\}$, the test output variables, is re-assigned in to one single cell array $O\{s\}$, then re-ordered in matrix order 8×12, for it to be displayed as result to the user.

Figure 6 shows the detailed system architecture of the reader system and a sample result along with the feature space of Test 5 with its centroids calculated by k-means clustering algorithm of the sample input image. There were no errors in classification by this technique for classifying the fluorescein concentrations that simulates the liquid transport assay, when Digital Camera was used for image acquisition; also paved the way for the usage of live samples such as Pathogens. Analyzing the variability introduced by a microorganism will lead to the incorporating changes to the algorithm of this reader system.

4 Results and Discussion

The suitability of k-means clustering technique for microtiter plate reader, which is a two-class pattern recognition application, depends on its accuracy and reproducibility. The classifier's accuracy was 100% when tested with 20 microtiter plate images having a dataset of 1920 sub-images. In addition, the computational complexity of the k-means algorithm was overcome by reducing the dataset from 96 observations of a single image to 6 groups with 16 observations in each group in a single classification process which was discussed in Section 3.2 and Section 3.3. Since the classification of the reader was accurate and reproducible, an experiment is necessary to find when the accuracy deters. The experiment was carried out by using four test images differed only by the source excitation intensity.

As in Figure 2, the circuit of the SMD3528 blue LED uses a square trim potentiometer of resistance range 2k for intensity control. The electrical travel of the moving arm inside this 2k square trim potentiometer causes the variation in the driver current of the circuit due to change in its resistance, which in turn controls the luminous intensity of the source. The resolution having total pixels around 9 megapixels and the image size are same in all four different test images by the same imaging hardware, here a digital camera. The acquisition conditions of the test images are in detail as followed.

A blue filter placed below the microtiter plate filters the source. In addition, 0% electrical travel of the 2k square trim potentiometer allows maximum drive current to the circuit providing maximum luminous intensity of

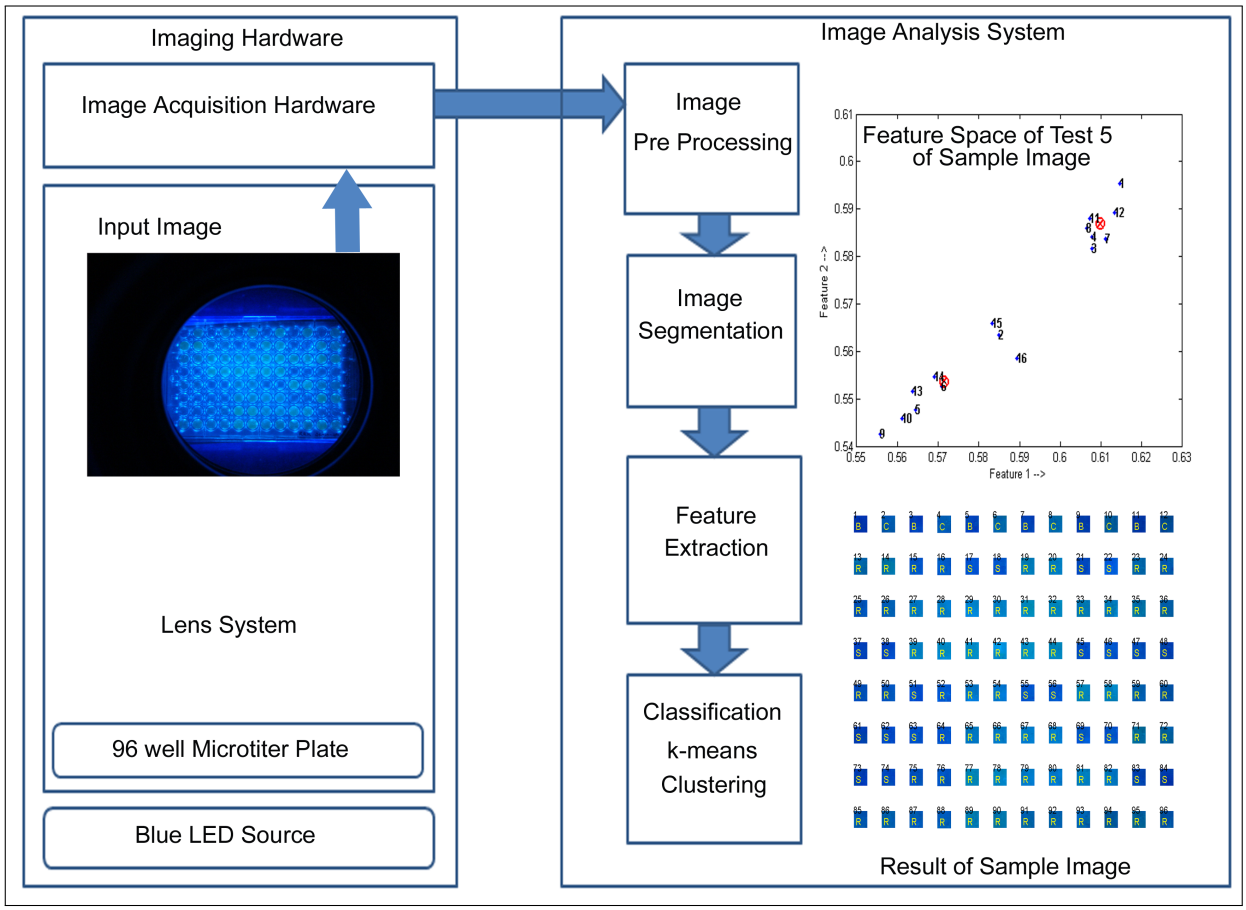

Figure 6: System Architecture of Microtiter Plate Reader System with Sample Analysis Process.

the source to the microtiter plate. Then the image acquired with these conditions by the digital camera having 9 megapixels CMOS sensor is the Test image 1. As of for Test image 2, the conditions of Test image 1 are retained except for the change in the filtration of the excitation source which is, placing a green filter above the microtiter plate along with the blue filter placed below it. Test image 3 has the conditions of the Test image 2 with change only in the luminous intensity of the excitation source. The change was to alter the electrical travel from 0% to 30% 2kΩ square trim potentiometer causing reduction in the luminous intensity of the excitation source and acquire it as an image. For the Test image 4, the change from Test image 3 is only in electrical travel from 30% to 50% of the intensity controlling 2kΩ square trim potentiometer.

Figure 7 shows the Test Images 1 to 4 fed to the reader system as inputs. The Table 2 shows the classification accuracy for the test images fed as input to the developed system. From the Table 2 we see that Test images 1 and 2 offer an accuracy of 100% and reduced accuracy of other two images due to the decrement in the excitation intensity. Hence, we can deduce that an efficient classification by this technique for this application, will be achieved, if and only if with maximum intensity provided by the blue LED source and the quality of the image is retained with high resolution.

The usage of a statistical classifier such as k-means clustering have been effective in this is two-class pattern recognition application, even though the size of the classes varies. Although class discrimination in this application was challenging, the effectively selected feature space after the feature selection has overcome this and provided a good dataset to k-means algorithm leading to the development of an efficient microtiter plate reader. Computational statistical technique employed for the processes of feature selection, feature extraction, and classification from the sub-images of a single microtiter plate image had given an advantage of simplicity to the system. The algorithm of the reader has the facility to alter to the change incorporated in need of the requirement. The requirement for alterability are mentioned here, the format of microtiter plate used, automation of imaging, image segmentation, number of classes in classification, and change in the feature space.

In this image based analysis, quantification by microtiter assays is dependent on the resolution of the image acquisition system as well as the image analysis method. However, method as the one described will be of great value for those assays having two-class classification problem such as appearance or disappearance of fluorescence or a broad gradation of color intensity deciding the analyte's range of concentration in a semi quantitative man-

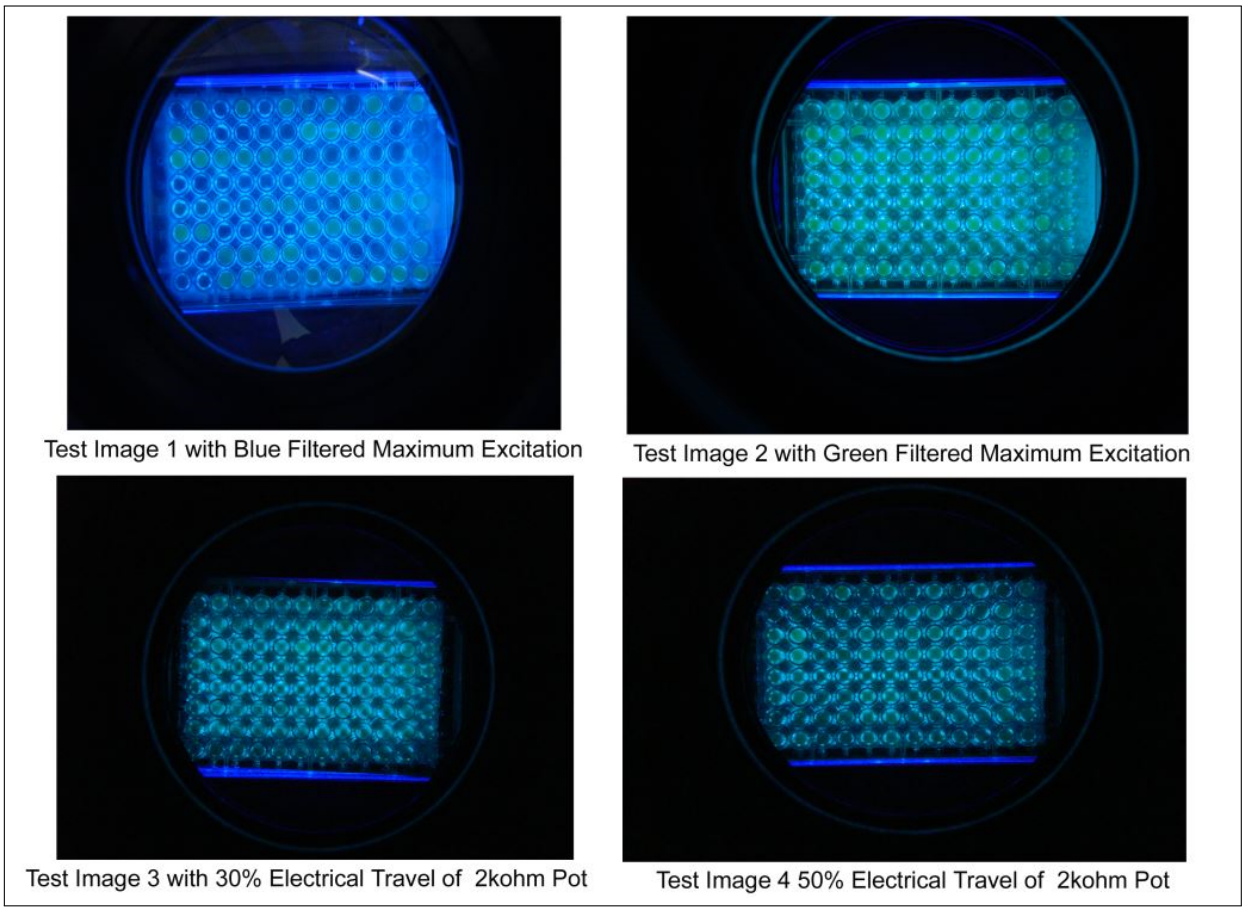

Figure 7: Test Images 1 to 4 of different Fluorescence Assays used for Performance Determinaton.

ner. When the image acquisition and software analysis are in perfect, the system could come close to the currently available scanning mode reader's performance with the decisive advantage of low cost, a big boon to clinical world.

5 Conclusions and Future Work

With the uniform illumination analysis and its dependency in degradation of classification performance, for this fluorescence assay it is deduced that, the SMD 3528 blue LED is suitable as source for this application, along with k-means clustering as the classification technique. This microtiter plate reader provides the maximum accuracy is achievable only when intensity of blue LED is maximum and the image quality retained as provided by a 9 megapixel-imaging sensor. The Future work is to experiment with low imaging sensor acquisition hardwares. In addition, to the above the goal is to achieve automation on imaging, image analysis and report generation. In addition, the assay when excited by the wavelengths in the visible-spectrum, captured as an image reduces the complexity in need of any heavy equipment. This reader system focused only on the 96-well format and easily alterable to any format, which is an advantage to this system. Thus using an image analysis system for such biotechnological assay reduces the time consumption, increases the efficiency, and converts all information to electronic data. The proposed imaging and image analysis system is very essential in the health care facilities due to its low complexity and cost effectiveness.

Table 2: Classification Accuracy of Different Assays.

Assay	Specificity %	Sensitivity %	Accuracy %
Test Image 1	100	100	100
Test Image 2	100	100	100
Test Image 3	97.92	97.92	97.92
Test Image 4	93.75	93.75	93.75

Acknowledgements

University Grants Commission (UGC), Government of India is acknowledged for financial support for the project in "Centre with Potential for Excellence in Environmental Science (CPEES), Anna University" and for the Fellowship of Junior Research Fellow to Durai Arun.

References

[1] Vecht-Lifshitz SE, Ison AP, "Biotechnological applications of image analysis: present and future prospects", Journal of Biotechnology, Volume 23, Issue 1, March 1992, Pages 1–18

[2] Gonzalez, Digital Image Processing, 2nd Edition, Pearson Education Inc., 2008

[3] Schalkoff, Artificial Neural Networks, McGrahill Publications, 1997

[4] Earl Gose, Richard Johnsonbaugh, Steve Jost, Pattern recognition and Image Analysis, Prentice Hall PTR, 1996

[5] Wendy L. Martinez, Angel R. Martinez, Computational Statistics Handbook with MATLAB, Chapman HALL/CRC, 2002

[6] Anil K Jain, Fundamentals of Digital Image Processing, Pearson Education, Inc., 1989.

[7] Muttan S, Durai Arun P, Sankaran K "Image Analysis System for 96-well Plate Fluorescence Assays" in the Proceedings of Third International Conference on Computing Communication Networking Technologies (ICCCNT 2012), Coimbatore, July 2012

[8] Karthik G, Muttan S, Sankaran K "Optical Viewing System for 96 well Plate using Transilluminator" in Proceedings of Sixth National Conference on Recent trends in Information Technology and Communication, Chennai, pp 71-73, April 2012

[9] Metin N. Gurcan, Anant Madabhushi, , Nasir M. Rajpoot, and Bulent Yener, "Histopathological Image Analysis: A Review," IEEE Reviews In Biomedical Engineering, Vol.2, pp. 147-171, 2009

[10] Le Jing, Li Yun, Hua Dengxin, Tan Linqiu, Cao Ning "Research on method of LED-induced chlorophyll fluorescence spectrum and image information acquisition" in the Proceedings of The Tenth International Conference on Electronic Measurement Instruments (ICEMI 2011)Pp. 311-315, 2011

[11] Timothy, Transilluminator, U.S. Patent No. 5347342 issued at September 13, 1994, Available at (http://www.google.com/patents/US5347342)

[12] Lei Li, Jin-Yan Li, Wen-Yan Ding. "A New Method For Color Image Segmentation Based on FSVM", In Proceedings Of The Ninth International Conference On Machine Learning And Cybernetics, Qingdao, Pp. 664-779, 2009

[13] Schalkoff, Pattern Recognition, 1st Edition, John Wiley Sons, 1992.

[14] Anil K Jain, M.N. Murthy, P.J. Flynn, "Data Clustering: A Review", ACM Computing Surveys, Vol. 31, No. 3, pp. 264-323, September 1999

[15] G.Chamundeswari, G. Pardasaradhi Varma, Ch. Satyanarayana "An Experimental Analysis of K-means Using Matlab", International Journal of Engineering Research Technology (IJERT) ISSN: 2278-0181Vol. 1 Issue 5, July 2012

[16] Surasit Songma Witcha Chimphlee Kiattisak Maichalernnukul Parinya Sanguansat "Classification via k-Means Clustering and Distance-Based Outlier Detection" in Proceedings of Tenth International Conference on ICT and Knowledge Engineering, Pp. 125-128, 2012

[17] G.Subramanya Nayak Ottolina Davide Puttamadappa C "Classification of Bio Optical signals using K- Means Clustering for Detection of Skin Pathology" International Journal of Computer Applications (0975 – 8887) Volume 1 – No. 2 Pp 92-96

